Int. J. Heat Mass Transfer. Vol. 26, No. 12, pp. 1857–1865, 1983
Printed in Great Britain

0017-9310/83 $3.00 + 0.00

HEAT TRANSFER FROM ROUND IMPINGING JETS TO A FLAT PLATE

PETER HRYCAK
Department of Mechanical Engineering, New Jersey Institute of Technology, Newark, NJ 07102, U.S.A.

(*Received* 16 *November* 1982 *and in revised form* 14 *April* 1983)

Abstract—An investigation of heat transfer from round jets, impinging normally on three instrumented flat plates, for various nozzle-to-target plate distances, with Reynolds numbers ranging from 14 000 to 67 000, and nozzle diameters from 3.18 to 12.7 mm, has been carried out. The experimental data at the stagnation point were given particular attention. Flat plate stagnation point data and the average heat transfer have also been correlated by means of dimensional analysis, and compared with calculations and with the results from the literature.

NOMENCLATURE

a^*	slope of dimensionless velocity profile plotted vs dimensionless distance from stagnation point, $\Delta(v/u_{oc})/\Delta(x/D)$ at $x = 0$
c_p	specific heat at constant pressure [J kg^{-1} K^{-1}]
C_f	friction coefficient
D	nozzle diameter [mm]
D_c	calorimeter diameter [mm]
D_p	plate diameter [mm]
h	heat transfer coefficient [W m^{-2} K^{-1}]
k	thermal conductivity [W m^{-1} K^{-1}]
L	significant length [mm]
Nu	Nusselt number, hD/k
Pr	Prandtl number, $c_p\mu/k$
r	distance from nozzle centerline [mm]
Re_D	Reynolds number, $u_{oc}D/v$
St	Stanton number, $Nu/(Re\ Pr)$
u	axial velocity [m s^{-1}]
v_s	radial velocity at stagnation point [m s^{-1}]
v	radial velocity, wall jet velocity [m s^{-1}]
x	distance away from stagnation point along target plate [mm]
z	distance away from target plate [mm]
Z_n	distance from nozzle to the target plate [mm].

Greek symbols

δ	boundary-layer thickness [mm]
δ^*	displacement thickness [mm]
θ	momentum thickness [mm]
μ	dynamic viscosity [kg (ms)$^{-1}$]
ν	kinematic viscosity [m^2 s^{-1}]
ρ	density [kg m^{-3}]
τ_w	wall shear stress [N m^{-2}].

Subscripts and other symbols

c	center of symmetry
D	dimensionless parameter with D as significant length
m	condition where velocity is a maximum
o	origin or stagnation point
oc	origin of jet at center of nozzle
s	conditions at surface of calorimeter
$\bar{}$	average (mean integral) value.

INTRODUCTION

ROUND jets impinging on heated/cooled surfaces, held normal to the axis of flow, are very attractive in a variety of cooling/heating applications because, in comparison with the heat transfer rates obtainable by ordinary methods of convective cooling or heating, a substantial increase in heat transfer coefficients can be realized with their use.

Impinging jets have recently attracted many investigators because of their eminent suitability to increase local heat and mass transfer. The earlier results on heat transfer from impinging jets have been summarized by Livingood and Hrycak [1], and by Martin [2]. An early experimental study of round impinging turbulent jets was carried out by Gardon and Cobonpue [3] and Gardon and Akfirat [4]. At the stagnation point [3, 4], the maximum local Nusselt number, Nu_o, was found to occur at $6 < Z_n/D < 7$, explained by an attenuation of the original jet nozzle velocity, u_{oc}, with the distance, within the 'potential core' extending from six to seven diameters downstream from the nozzle exit [5], and a strong turbulence pattern in the mixing region at the tip of the potential core. For $Z_n/D < 6$, secondary peaks away from the stagnation point were observed in local heat transfer coefficients, thought to be related to the hydraulic jump phenomenon and the transition from stagnation flow to the wall-jet flow. Round turbulent air jets impinging on a heated segmented flat plate consisting of six concentric flat Invar rings were studied by Chamberlain [6]. Datta [7] carried out similar measurements on a flat plate with embedded calorimeters, investigating the effect of the nozzle diameter and of Z_n/D on the Nusselt number.

Because the governing equations are similar, it is often helpful to use mass transfer measurements to study heat transfer from impinging jets, cf. Schrader [8], who used an experimental set-up somewhat similar to a

segmented flat plate. Schrader found the surface finish of the target plate to be a significant independent variable in his correlation, as also did Sakipov *et al.* [9] more recently. Also, important are the physical details of the nozzles used.

Among the nozzles used, one can consider two extremes: on one hand, tube-type nozzles (used in refs. [3, 6]), where there occurs a large degree of mixing of the jet with the surrounding air, and on the other hand, simple orifices made in a wall parallel to the target plate, where the mixing with ambient air is restricted. Most nozzles used in the literature fall somewhat into the middle between these two extremes [1, 2]. Tube-type nozzles with an internal lip at the exit have been used in this paper and in ref. [7].

Impinging jets may be used for both cooling and heating purposes, but entrainment of ambient temperature fluid by the impinging hot jet will reduce its heating effectiveness, except for short nozzle-to-plate distances. Stagnation point heat flux from hot impinging jets was measured by Comfort *et al.* [10] and by Vlachopoulos [11]. Schrader [8] used warm jets in his mass transfer measurements.

As is seen from refs. [1–4], the fluid flow characteristics of impinging jets determine their heat transfer effectiveness, as also discussed, for example, by Shvets and Dyban [12] and Dyban and Mazur [13]. Sibulkin [14] obtained a theoretical solution for the stagnation point heat transfer, good for a low velocity axisymmetric jet impinging on a flat surface. A systematic study in ref. [13] of jets that had definitive, artificially induced turbulence levels (up to $Tu = 28\%$), produced at the stagnation point results that were up to 100% higher than those indicated by Sibulkin's formula, while ref. [4] indicated that some of the naturally occurring jets had already turbulence levels in the range of Tu investigated in ref. [13]. Therefore, in practical applications stagnation point heat transfer may be expected to be higher than that predicted by ref. [14], and it would be desirable to develop here expressions in a better agreement with the experimental data. From the study of the applicable review literature [1, 2], and of the monograph by Schlichting [15], it appears that heat transfer from impinging jets to flat plates requires still a lot of additional experimental and analytical work. Since the available theory is still incomplete [14, 15], and for a better comparison of experimental data of various investigators and analysis of the present data, dimensional analysis, and semi-empirical correlations based on dimensional analysis are very helpful.

Thus, for the local value of the Nusselt number, Nu, we can expect, from the consideration of all the contributing variables for heat transfer from impinging jets, a relation involving Re_D, Pr, and six characteristic linear dimensions; the required functional form, strictly applicable only for the specific ranges of the independent parameters investigated, may be approximated here by the expression (which, in turn, may be only piecewise continuous)

$$Nu = K\, Re_D^a\, Pr^b\, (Z_n/D)^c (\bar{D_c}/D)^d (D_p/D)^e (x/D)^f (L_1/D)^g, \quad (1)$$

where K, a, b, c, etc., are considered constants over the restricted ranges of the major independent variables, that can be evaluated either theoretically or experimentally; this $a = 0.5$ applies in the stagnation region, according to ref. [14] and $a \approx 0.7$ in the wall-jet region; where $x \approx 0$ and $f = 0$ applies, Nu reduces to Nu_o. Equation (1) has been normalized with the help of the nozzle diameter D, considered here to be the most significant characteristic linear dimension, but other combinations can be found in the literature, e.g. based on D_p and D_c [1, 2, 8]. The unspecified term L_1 may be specialized according to the need; for example, L_1 may be associated with the sand-grain diameter characteristic of a particular surface [8].

This paper intends to fill the need for additional heat transfer data from impinging jets by presenting a large number of experimental results obtained from direct heat transfer measurements in the steady state, while using a variety of heat transfer transducers and experimental arrangements, for the Reynolds numbers (based on the diameter of the nozzle and air properties at the nozzle exit), ranging from 14 000 to 67 000, and the nozzle diameter D of 3.18, 6.35, 9.52 and 12.7 mm. The general experimental approach taken is similar to the techniques described in two other papers [16, 17], that dealt with jets impinging internally on a cylindrical and a hemispherical target plate, respectively.

EXPERIMENTAL TEST SET-UP

The jet was directed normally towards the center of the target plates, all of 152.4 mm in diameter (Fig. 1), heated from below by steam condensing at atmospheric pressure. Air, filtered and dehumidified, was supplied by a reciprocating compressor with a large settling tank and sent to the plenum chamber, to equalize the flow. Air volume was measured with two rotameters, accurate to within 1% of the full scale reading. Interchangeable nozzles could be attached to the end plate of the plenum chamber. Originally, straight-bore tube nozzles were employed, as those in refs. [3, 6] and later on, tube-type nozzles with an inner lip at the exit (see Fig. 2), to provide a flat velocity profile, as shown in Fig. 5 (insert).

Plate A was a solid plate made of 304 stainless steel, 19 mm thick, supported by a 6.35 mm thick brass base plate, and equipped with 14 304 SS embedded calorimeters with diameters of 5.08 mm whose locations are indicated by crosses in Fig. 1. Calorimeter detail is shown in Fig. 4. Plate B, made of 304 SS, consisted of six concentric segments 18.6 mm thick, separated from each other by a 1.6 mm gap and supported by a 6.35 mm brass plate. The gap was sealed on top with a layer of silicone rubber. Plate C, 14.4 mm thick, made of Invar, was otherwise geometrically identical with plate B. The original version of plate C was also used by Chamberlain [6].

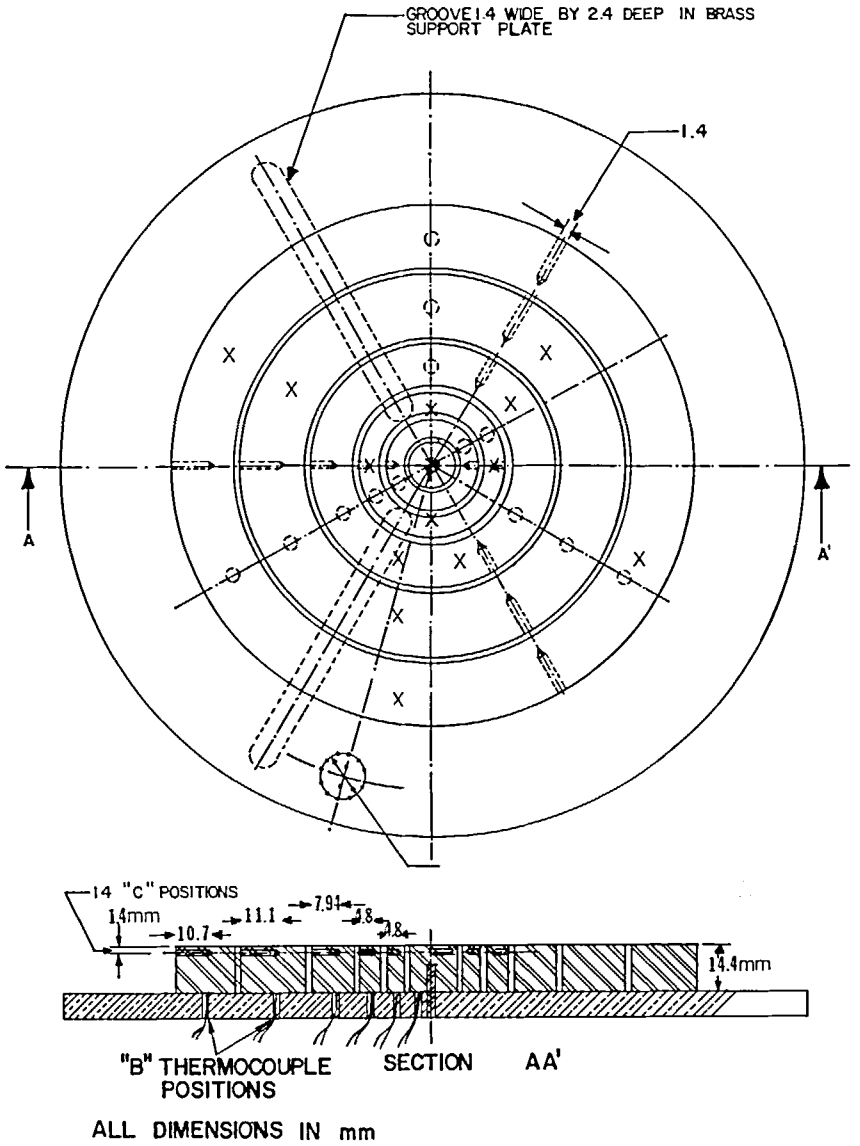

FIG. 1. (a) Segmented plate, top view; location of embedded calorimeters in solid 304 stainless steel plate. (b) Segmented plate, side view.

The particular metals chosen for the test plates were stainless steel and Invar because they are relatively resistant to oxidation, and may keep well their original surface finish. Also, they may represent roughly the behavior of alloys used in typical applications of jet cooling.

To measure heat flux, one set of thermocouples was mounted near the surface, and the other near the base of the individual plate segments. The center segment of each plate, interchangeable, acted as a kind of a center calorimeter. Eventually, individually calibrated constantan–copper thermocouples, made from 40 gauge wire, were adopted, to minimize the thermocouple conduction error, and the calorimeter diameter, D_c, was reduced to 5.08 mm for a better local heat flux resolution; for strictly one-dimensional heat flux, asbestos side insulation was employed with consistent results. Some bakelite-insulated calorimeter data are shown in Fig. 2. Bakelite had a tendency to swell with moisture and to short out the thermocouple circuits. Also, to minimize all contact resistances, silver-powder loaded grease was used on all places of contact.

Samples of the metal used for the calorimeters had their thermal conductivity tested individually by the electrical conductivity analogy method [18, 19], with an error of less than 3%. The conductivity of the 304 SS used agreed well with the literature, but that of Invar was found to be 40% higher (13.6 $Wm^{-1}K^{-1}$ at 273.15 K and 15.5 $Wm^{-1}K^{-1}$ at 373.15 K).

Heat transfer coefficients were calculated from the formula

$$h = -\left(\frac{k}{A}\right)(t_t - t_b)/(t_s - t_{air}),$$

$$t_s = t_t + (t_t - t_b)(B/A - 1). \quad (2)$$

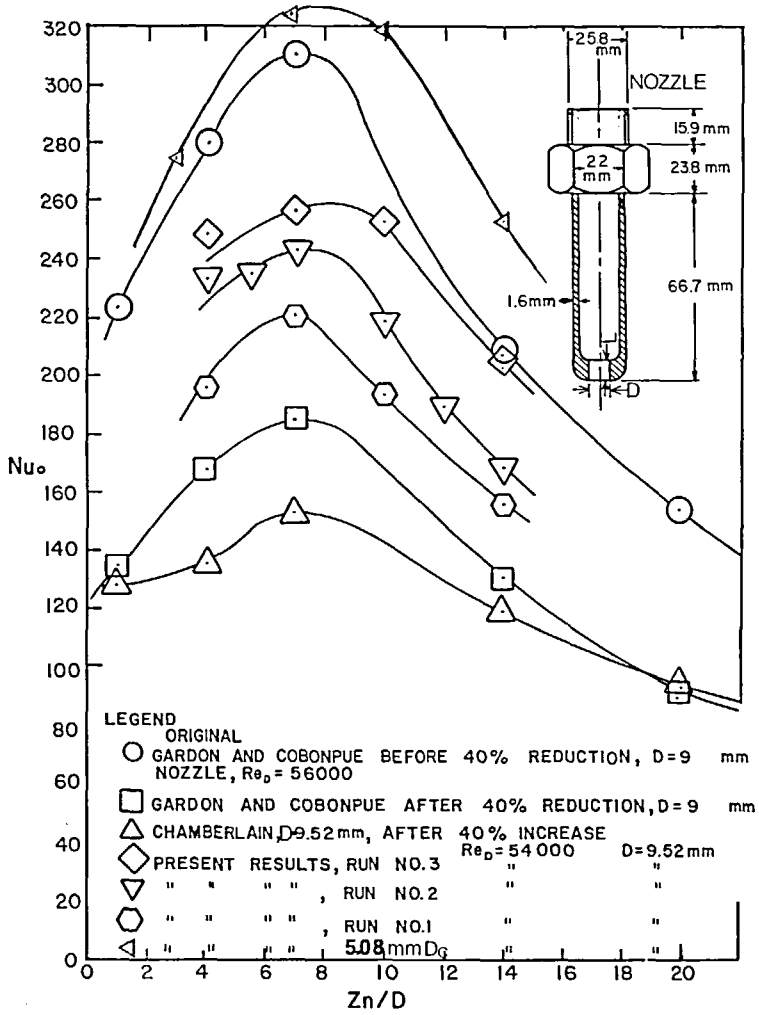

FIG. 2. Stagnation point results on plate C, with Invar center calorimeter. Calorimeter development progress and comparison with experimental results of Gardon *et al.* Results obtained with a 5.08 mm diameter calorimeter with bakelite side insulation. Detail of the lip-equipped nozzle.

where subscript b refers to the bottom thermocouple, t to the top thermocouple, A is the distance between t_t and t_b, and B is the distance between t_s and t_b. The total calorimeter error is calculated as being less than 5% for the calorimeter shown in Fig. 4. This error is due to the contact resistance and the thermocouple lead conduction, to the effect of the holes drilled to accommodate the thermocouples on the overall conductance of the calorimeter, and the conductivity measurement error.

EXPERIMENTAL RESULTS

Before final, representative results were achieved, some experimentation with the transducers used for heat flux measurements was necessary. In Fig. 2 the present stagnation point results are compared with those by Gardon and Cobonpue [3] and by Chamberlain [6]. It is seen that, as the contact with the brass support plate was improved (Run 1), and the thermocouple wire conduction error eliminated (Runs 2 and 3), the measured intensity of heat transfer was found to increase, and Run 3 results come out quite close to the original measurements in ref. [3]. All results show a maximum near $Z_n/D = 7$. In Fig. 2, data points for Runs 1–3 were obtained both with lip-equipped nozzles and straight-bore tubes of the same length (see detail in Fig. 2), but no significant differences in results were found. Plates A–C were then tested extensively with the results shown in Fig. 3. For the final stagnation point tests in plates B and C, the center segment with a diameter of 11.1 mm was replaced by a 5.08 mm diameter calorimeter with a 2.54 mm layer of asbestos on the side (see Fig. 4), with the length to match the height of each plate, and made both in Invar and 304 SS versions. Using, for example, the symbol A_{ss}, for plate A with 304 SS calorimeters, etc., combinations tested were A_{ss}, B_i, B_{ss}, C_i, and C_{ss}, to eliminate the systematic errors possible in the calibration and manufacturing of heat flux transducers, occasionally reported in the literature [4]. The stagnation point results, shown in

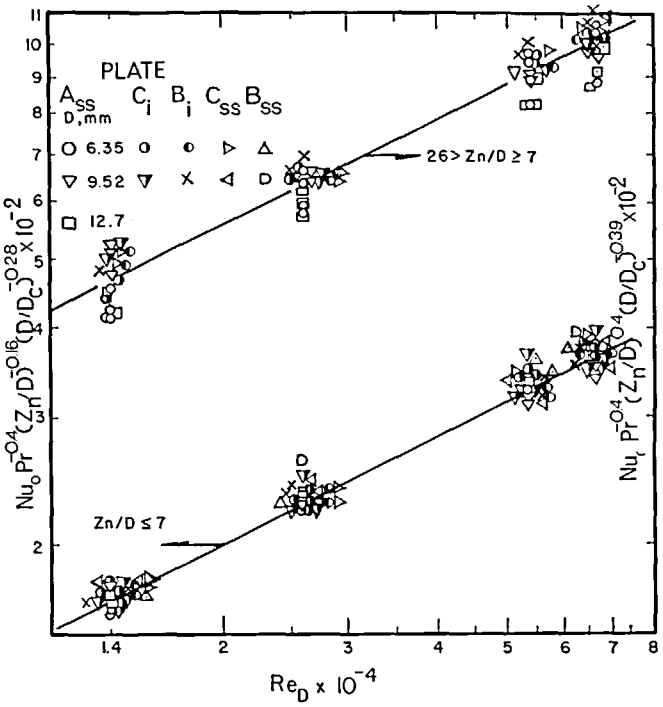

FIG. 3. Stagnation point heat transfer results for all three flat plates investigated: plate A with embedded 304 SS calorimeters (A_{ss}); plate B with Invar center calorimeter (B_i), plate B with 304 SS center calorimeter (B_{ss}); plate C with invar center calorimeter (C_i), and plate C with 304 SS calorimeter (C_{ss}).

Fig. 3, may be correlated for $Z_n/D < 7$ by the expression

$$Nu_o = 1.41\ Re_D^{1/2}\ Pr^{0.4}\ (Z_n/D)^{0.16}(D/D_c)^{0.28}, \quad (3)$$

which shows that Nu_o increases with Z_n/D for tube-type nozzles (cf. refs. [3, 6, 7]), and the explicit effect of D on Nu_o for heat flow within the potential core, while for $Z_n/D > 7$

$$Nu_o = 3.92\ Re_D^{1/2}\ Pr^{0.4}\ (Z_n/D)^{-0.4}(D/D_c)^{0.39}, \quad (4)$$

indicates a decrease of Nu_o with the nozzle-to-target spacing outside of the potential core.

The average data, obtained through integration of

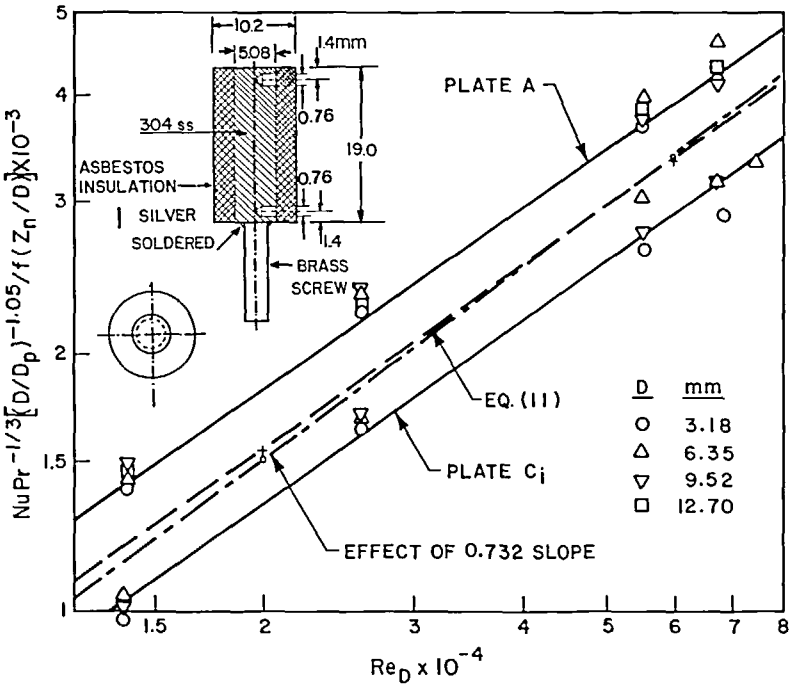

FIG. 4. Average results, solid 304 stainless steel plate (plate A), upper curve; average results, segmented Invar plate (plate C_i), lower curve; comparison with equation (11) results. 5.08 mm diameter calorimeter detail.

local values over the entire test plate, for plates A and C_i, are shown in Fig. 4. Plate A results correlate as

$$\overline{Nu} = 1.85\, Re_D^{0.695}\, Pr^{0.33}\, (D/D_p)^{1.05} f(Z_n/D), \quad (5a)$$

while plate C_i data yield the expression

$$\overline{Nu} = 1.32\, Re_D^{0.7}\, Pr^{0.33}\, (D/D_p)^{1.05} f(Z_n/D), \quad (5b)$$

where $f(Z_n/D) = (7D/Z_n)^{0.17}$ for $Z_n/D > 7$, while $f(Z_n/D) \equiv 1$, if $Z_n/D < 7$.

Since the overall experimental arrangements in both cases were nearly identical, the only conceivable reason for the difference between results for plates A and C_i appears to be in the effective roughness of the plates tested. Equations (5a) and (5b) show many similarities, but they also indicate clearly the importance of surface finish on heat transfer with impinging jets, as observed already in refs. [8, 9].

DISCUSSION OF RESULTS

Heat transfer at the stagnation point is shown in Figs. 2 and 3. In Fig. 2, it is interesting to note that the range of Nusselt values between the original Gardon and Cobonpue results [3] and those obtained after 40% reduction due to uncertainties in the transducer calibration [4] is very similar to the spread of the data lying between Chamberlain's results, and those obtained in the present investigation with the bakelite-insulated calorimeter. Figure 2 shows how consistent improvements in the design of the transducers used helped to produce more reliable physical measurements.

Also, it is seen from Fig. 2 that the heat transfer intensity has the tendency to peak out at $Z_n/D \approx 7$ at the point of impingement, for tube-type nozzles. It is thus following the turbulence patterns associated with the attenuation of the potential core of the jet [4]. From equation (3) and Fig. 3 the heat transfer coefficient at the stagnation point may be estimated as 1300–1500 $W\,m^{-2}\,K^{-1}$ for $D = 9.52$ mm and $Re_D = 67\,000$; this is about 30% higher than a similar result in ref. [3], but quite modest in comparison with the fluxes cited in ref. [12] and of a similar order of magnitude as results in refs. [10, 11] for heated jets.

Equation (3) is very similar to a formula obtained by Schrader [8] which, adopted for a surface of average smoothness, assumes in the present notation the form, good for $x \leqslant 0.9\, D$

$$Nu_o = 1.53\, Pr^{0.34}\, Re_D^{1/2}\, (Z_n/D)^{-0.2} (a^*)^{1/2}, \quad (6)$$

valid for $Z_n/D < 10$. Due to a different nozzle design, the Z_n/D dependence of equation (6) is similar to the formula for Nu_o obtained in ref. [16], for jets formed by sharp-edged orifices in a plate. In equation (6) $\frac{1}{2}D_p$ was originally the significant dimension, and $D_p = D_c$ also applied. An explicit dependence on D is not shown, although ref. [8] indicates that $Nu \propto D^{0.2}$. Vallis *et al.* [20] obtained from electrochemical mass transfer measurements for Nu_o an equation very similar to equation (6); other information in ref. [20] indicates also that $Nu_o \propto D$. Dimensional analysis suggests that $Nu_o \propto D$ if other linear dimensions remain unchanged, and D is varied; this is seen also from refs. [1, 3, 6–8, 20], and from equations (1) and (3); D_c dependence of equation (3) is valid only in the particular range of parameters investigated, however.

Equation (3) can also be obtained, from a relation between the momentum transfer and heat flux in the laminar sublayer (Appendix A)

$$Nu_o = 1.312\, Re_D^{1/2}\, Pr^{0.4}\, (a^*)^{1/2}. \quad (7)$$

The slope of the dimensionless velocity profile at the stagnation point, a^* can be obtained experimentally and approximated as $a^* \to 1$ when $Z_n/D \to 1$ [2, 8, 16]. Then, letting $D/D_c = 1$, equations (3) and (7) become nearly identical. Equation (4), for $Z_n/D > 7$, is obtained from equations (3) and (8) by introduction of the 'velocity of arrival', valid outside of the potential core [3, 5]

$$u_c = u_{oc} 6.6/(Z_n/D), \quad (8)$$

instead of u_{oc} into Re_D and readjusting the powers of Z_n/D and D/D_c for the minimum scatter of the data.

Equation (5), describing the average heat transfer, is dependent on the diameter ratio, D/D_p, which shows that the effect of the single jet is less pronounced when the flow spreads out over a larger plate. Because, for $Z_n/D < 7$, the target plate is on average still exposed to the full effect of the original jet velocity, the average Nusselt number is independent of Z_n/D, for $D_p/D \leqslant 48$.

Equation (5) can be reproduced from the formula for the wall-jet boundary-layer thickness [5]

$$\delta/D = 0.0175(x/D)^{0.95}, \quad (9)$$

and the corresponding maximum-velocity decay and velocity distribution expressions with $7.5 < n < 15$ within the wall-jet inner boundary layer ($z < \delta$)

$$v_m/u_{oc} = 1.4(x/D)^{-1.12},\ v/v_m = (z/\delta)^{1/n}. \quad (10)$$

These results, together with an appropriate expression for the wall friction coefficient C_f, (Appendix B), yield a formula that closely represents the average of equations (5a) and (5b)

$$\overline{Nu} = 1.5\, Re_D^{0.7}\, Pr^{0.33}\, (D/D_p)^{1.07}, \quad (11)$$

and forms a check on the validity of the present experimental results for $Z_n/D < 7$, with an estimated experimental error of $\pm 15\%$. The total heat transfer here, evaluated as 17 000 $W\,m^{-2}$ for $Re_D = 67\,000$, for example, is reasonable in comparison with the heat fluxes indicated by Shvets and Dyban [12]. The term $f(Z_n/D)$ in equation (5) is introduced to satisfy the average data outside of the potential core region ($7 < Z_n/D < 26$).

An investigation of heat transfer from a single, round, impinging jet may also be viewed as an intermediate step towards applications leading to jets impinging on targets with a more complex geometry [16, 17]. Mass transfer results have been very helpful in the

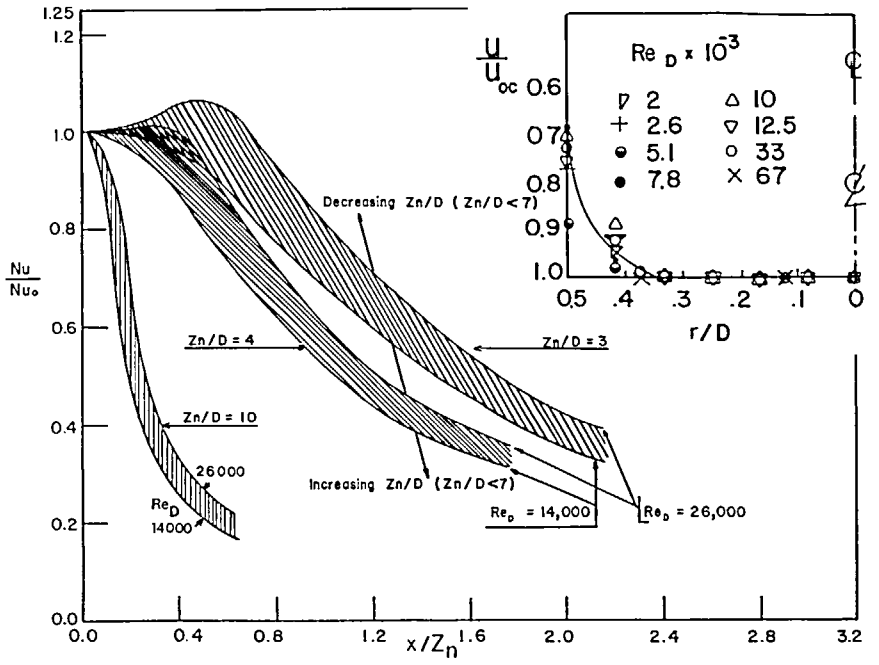

FIG. 5. Trends of local heat flux and impinging jets for a flat plate as a function of radial distance and the nozzle-to-target spacing x/Z_n (adapted from ref. [7]). Typical nozzle velocity profile for nozzle in Fig. 2.

explanation of many impinging jet heat transfer phenomena (cf. ref. [8]). It appears, however, that for the more complex geometries, together with high Reynolds numbers, direct heat transfer measurements will become a practical necessity, for producing heat fluxes close to their theoretical limit.

The local distribution of heat transfer coefficients, shown in the summary of experimental results in Fig. 5, indicates the complexity of the underlying physical phenomena here, and a need for additional research. The nozzles (Fig. 2) used in the present experiments were of the type that had relatively good flow characteristics as shown in Fig. 5, and were likely to resemble the ones used in the representative applications, produced at the stagnation point heat fluxes that peaked up at $Z_n/D \approx 7$ (cf. also refs. [3, 6, 7]), while 'orifice in the wall' type nozzles generated heat fluxes that monotonically decreased with Z_n/D [8, 16]. These two radically different kinds of nozzles here reflect the prevailing industrial practices and the particular needs of the processes where impinging jet heat transfer is of significance today.

CONCLUSIONS

Experimental results for heat transfer between a flat plate and impinging turbulent air jets have been presented, for conditions applicable both inside and outside of the potential core, for the stagnation point heat flux as well as for the average heat transfer obtained through integration of local heat fluxes.

Average heat transfer, while inside of the potential core, was shown to be essentially independent of the nozzle-to-plate spacing, but was influenced by the condition of the target plate surface and was inversely proportional to the diameter of the target plate.

The stagnation point results showed that the Nusselt number has a tendency to peak out about seven diameters away from the target plate, for tube-type nozzles used here. Semiempirical correlations of all results were also presented, showing the effect of the nozzle Reynolds number and other pertinent variables. At the stagnation point, there is a very pronounced Nusselt number dependence on the half power of the Reynolds number, indicating laminar boundary-layer flow, yet heat transfer intensity is higher than in the theoretical solution. Average heat transfer is influenced mainly by the heat flux in the wall-jet region, with dependence on the 0.7 power of the Reynolds number. The present experimental results, when compared with those in the references cited, fall into the middle between the cold and hot jet results, and are reasonably close to the representative mass transfer results discussed.

Acknowledgements—This project has been partially supported by grants NGR-31-009-004 and MEA 81-19471. C. S. Datta, Norman Shilling, D. Joseph and M. Furman helped with collection and processing of data.

REFERENCES

1. J. N. B. Livingood and P. Hrycak, Impingement heat transfer from turbulent air jets to flat plates—a literature survey, NASA TM X-2778 (1973).
2. H. Martin, Heat and mass transfer between impinging gas jets and solid surfaces, in *Advances in Heat Transfer* (edited by J. P. Hartnett and T. F. Irvine, Jr.), Vol. 13, pp. 1–60. Academic Press, New York (1977).

3. R. Gardon and J. Cobonpue, Heat transfer between a flat plate and jets of air impinging on it, in *International Developments in Heat Transfer*, pp. 454–460. ASME (1963).
4. R. Gardon and J. C. Akfirat, The role of turbulence in determining the heat transfer characteristics of impinging jets, *Int. J. Heat Mass Transfer* **8**, 1261–1272 (1965).
5. P. Hrycak, D. T. Lee, J. W. Gauntner and J. N. B. Livingood, Experimental flow characteristics of a single turbulent jet impinging on a flat plate, NASA TN D-5690, Washington, DC (1970).
6. J. E. Chamberlain, Heat transfer between a turbulent round jet and a segmented flat plate perpendicular to it. M.S. thesis, Newark College of Engineering, Newark, New Jersey (1967).
7. C. S. Datta, Cooling characteristics of a turbulent round jet impinging normally on a heated flat plate. M.S. thesis, Newark College of Engineering, Newark, New Jersey (1970).
8. H. Schrader, Trocknung feuchter Oberflächen mittels Warmluftstrahlen Strömungsvorgänge und Stoffübertragung, *VDI ForschHft.* **27B**, 484 (1961).
9. Z. B. Sakipov, D. B. Kozakhtov and L. I. Zubareva, Analysis of turbulent jets flowing over smooth and rough surfaces, *Heat Transfer–Soviet Res.* **7** (4), 125–137 (1975).
10. E. H. Comfort, T. J. O'Connor and L. A. Cass, Heat transfer resulting from the normal impingement of a turbulent high temperature jet on an infinitely large plate. *Proc. Heat Transfer and Fluid Mech. Institute*, pp. 44–62 (1966).
11. J. Vlachopoulos, Heat and momentum transfer in the compressible turbulent wall jet. Sc.D. dissertation, Washington University, St. Louis, Missouri (1969).
12. I. T. Shvets and E. P. Dyban, *Air Cooling of Gas Turbine Elements* (in Russian), Naukova Dumka, Kiev, U.S.S.R. (1974).
13. E. P. Dyban and A. J. Mazur, Heat transfer near stagnation point from turbulized impinging jets, *Thermal Physics and Thermal Technol.* No. 33 (in Russian), 6–11 (1977).
14. M. Sibulkin, Heat transfer near the forward stagnation point at a body of revolution, *J. Aeronaut. Sci.* **19**, 570–571 (1952).
15. H. Schlichting, *Boundary-Layer Theory* (7th edn.). McGraw-Hill, New York (1979).
16. P. Hrycak, Heat transfer from a row of impinging jets to concave cylindrical surfaces, *Int. J. Heat Mass Transfer* **24**, 407–419 (1981).
17. P. Hrycak, Heat transfer and flow plate characteristics of jets impinging on a concave hemispherical plate, *Proc. 7th Int. Heat Transfer Conf.*, Vol. 3, pp. 357–362. Munich (1982).
18. D. R. Flynn, Calculation of the thermal conductivity of an Invar sample from electrical resistivity data, NBS Report 9655 (1967). (Obtainable from the author.)
19. D. R. Flynn, Thermal conductivity and electrical resistivity of a sample of AISI type 304 stainless steel, NBS Report 9869 (1968). (Obtainable from the author.)
20. E. A. Vallis, M. A. Patrick and A. A. Wragg, Radial distribution of convective heat transfer coefficient between an axisymmetric jet and a flat plate held normal to the flow, *Proc. 6th Int. Heat Transfer Conf.*, Vol. 5, pp. 297–303. Toronto (1978).
21. H. Ludwieg and W. Tillmann, Untersuchungen über die Wandschubspannung in turbulenten Reibungsschichten, *Ing.-Arch.* **17**, 288–299 (1949).

APPENDIX A

DERIVATION OF NUSSELT NUMBER AT STAGNATION POINT, Nu_s

Experimentally obtained expressions for heat transfer at the stagnation point exhibit both laminar and turbulent flow characteristics. To the first category belongs the half power of the Reynolds number [cf. equation (3)], indicating clearly the laminar boundary-layer flow, as well as the measurements related to the boundary-layer thickness [5, 16]. Still, the measured heat transfer rates are consistently higher than those given by Sibulkin's equation [14]. It is believed, therefore, that at the stagnation point, the following reasoning may shed some light on the problem. Note that, in the terms below, the primes on k and μ indicate the influence of turbulence on molecular conduction here in the boundary layer: shear stress is $\tau = \mu'(\mathrm{d}v/\mathrm{d}z)$, and heat transfer $q/A = -k'(\mathrm{d}T/\mathrm{d}z)$. Their ratio is, after letting $k'/\mu' = c_p Pr^{-m} Re^{-n}$, where the exponents m and n are yet to be determined experimentally

$$(q/A\tau) = -c_p\, Pr^{-m}\, Re^{-n}\, \mathrm{d}T/\mathrm{d}v. \tag{A1}$$

On separation of variables and integration ($v = v_s$ at $T = T_\infty$, $v = 0$ at $T = T_w$) while keeping $q/\tau = q_w/\tau_w = \text{const.}$, one obtains

$$q_w v_s/A\tau_w = c_p(T_w - T_\infty)\, Pr^{-m}\, Re^{-n}, \tag{A2}$$

with $q_w/[A(T_w - T_\infty)] = h$; after dividing by ρv_s^2, it gives

$$\frac{h}{c_p \rho v_s} = \frac{\tau_w}{\rho v_s^2}\, Pr^{-m}\, Re^{-n}, \tag{A3}$$

or

$$St\, Pr^m\, Re^n = C_f/2,$$

where the Stanton number is defined as $St = (hD/k)/(Pr\, v_s D/\nu)$ and $v_s = ax$, the potential flow velocity at the stagnation point. Now, from Froessling's solution [14], $\mathrm{d}^2\phi(0)/\mathrm{d}\zeta^2 = 1.312$. Since $\mathrm{d}\phi/\mathrm{d}\zeta = v/v_s$, and $\zeta = \sqrt{(a/\nu)}z$, one can write $C_f/2 = (\mu/\rho)\,\hat{c}(v/v_s)/\hat{c}(zv_s) = 1.312\,(a\nu/v_s^2)^{1/2} = 1.312\,[\sqrt{(a^*/Re_D)}]\,(u_\infty/v_s)$, with $a^* = aD/u_\infty$. Consequently, with $m = 0.6$, and $n = 0$, in analogy to results in refs. [1, 2, 14], and equation (3), one gets for flow of a gas with Pr close to unity

$$Nu_{s,D} = 1.312\, Re_D^{1/2}\, Pr^{0.4}\, \sqrt{a^*}, \tag{A4}$$

which is sufficiently close to the experimentally obtained values on the flat plate, equation (3), for $Z_n/D \to 1$ and $D \geqslant D_c$, while the exact theoretical solution [14] represents actually the lower limit for a 100% laminar, stagnation point flow:

$$Nu_{s,D} = 0.763\, Re_D^{1/2}\, Pr^{0.4}\, \sqrt{a^*},$$

where the numerical constant is proportional to $[\mathrm{d}^2\phi(0)/\mathrm{d}\zeta^2]^{1/3}$, and is 42% lower. The form of C_f used above, justified by the essentially laminar character of the flow near the stagnation point found experimentally [5], is also suggested by the measurements of the boundary-layer thickness there [16] and is similar to equation (21-55a) in Schlichting [15] applicable to all similar solutions in the Falkner–Skan flow; equation (A4) is likewise related to equation (12-56), *ibid.*, and is an example of the laminar boundary-layer techniques extendable to turbulent flows [15, p. 289].

APPENDIX B

DERIVATION OF AVERAGE NUSSELT NUMBER IN THE WALL JET REGION

The use of the Colburn analogy, with $f(Pr) = Pr^{2/3}$, and of a suitable friction coefficient, makes it possible to calculate heat transfer in the wall jet region. Therefore, let us try $C_f/2 = 0.123\,(v_m'\theta/\nu)^{-0.268} 10^{-0.678\delta^*/\theta}$, a formula due to Ludwieg and Tillmann [21]. The displacement thickness is defined here as

$$\delta^* = 2\int_0^\delta (1 - v/v_m)x\, \mathrm{d}z/D_p, \tag{B1}$$

in a form appropriate for axisymmetric flow, and likewise, the momentum thickness is

$$\theta = 2\int_0^\delta (v/v_m)(1 - v/v_m)x\, \mathrm{d}z/D_p. \tag{B2}$$

One can further define the Stanton number $\equiv (hD/k)/(Pr$

$v_m D/\nu$). Through substitution of expressions for v/v_m, v_m and δ applicable to axisymmetric wall-jet flow [equations (9) and (10) with $n = 14$] into the L–T formula, one gets $C_f/2 = 0.0206 (v_m\theta/\nu)^{-0.268}$. This form of $C_f/2$, set equal to $St\ Pr^{2/3}$, generates here the local Nusselt number for the wall jet, that integrated over the entire plate, and divided by $\pi D_p^2/4$, results in

$$\overline{Nu} = 1.07\ Re^{0.732}\ Pr^{1/3}(D/D_p)^{1.074},$$

where for $14\,000 < Re_D < 67\,000$ is equivalent within $\pm 3\%$ to

$$\overline{Nu} = 1.50 Re_D^{0.7}\ Pr^{1/3}(D/D_p)^{1.074}. \quad \text{(B3)}$$

Equation (B3) includes the effects of the experimentally determined terms v_m and δ, and of the correct inner-layer velocity profile. The error in extending the wall-jet region down to $x = 0$ is less than 4%.

TRANSFERT THERMIQUE POUR DES JETS CIRCULAIRES FRAPPANT UNE PLAQUE PLANE

Résumé—Cette étude concerne le transfert thermique pour des jets circulaires frappant normalement trois plaques planes avec des distances variables entre orifice et plaque, des nombres de Reynolds compris entre 14 000 et 67 000, des diamètres d'orifice entre 3,18 et 12,7 mm. Les données expérimentales correspondant au point d'arrêt sont précisées avec une attention particulière. Les données au point d'arrêt et le transfert thermique moyen ont été représentés par le moyen de l'analyse dimensionnelle et elles sont comparées avec les calculs et avec les résultats disponibles dans la littérature.

WÄRMEÜBERGANG VON RUNDEN STRAUSTRAHLEN AN EINER EBENEN PLATTE

Zusammenfassung—Eine Untersuchung des Wärmeübergangs von runden Strahlen, die senkrecht auf drei ebene Meßplatten auftreffen, wurde für verschiedene Abstände der Düse zur Platte mit Reynolds-Zahlen zwischen 14 000 und 67 000 und Düsendurchmessern von 3,18 bis 12,7 mm durchgeführt. Den experimentellen Werten am Staupunkt wurde besondere Aufmerksamkeit gewidmet. Die Versuchsdaten am Staupunkt für die ebene Platte und der mittlere Wärmeübergangskoeffizient wurden mit Hilfe der Dimensionsanalyse korreliert und mit Berechnungen und Ergebnissen aus der Literatur verglichen.

ПЕРЕНОС ТЕПЛА ОТ НАТЕКАЮЩИХ НА ПЛОСКУЮ ПЛАСТИНУ КРУГЛЫХ СТРУЙ

Аннотация—Исследуется перенос тепла от круглых струй, натекающих под прямым углом на три снабженные датчиками плоские пластины, находящиеся на различных расстояниях от сопла, в диапазонах изменения числа Рейнольдса от 14000 до 67000 и диаметра сопла от 3,18 до 12,7 мм. Особое внимание обращено на экспериментальные данные, полученные в критической точке. С помощью анализа размерности выявлена взаимосвязь между этими данными и средними значениями коэффициентов теплопереноса и проведено сравнение с опубликованными результатами расчетов и опытными данными.